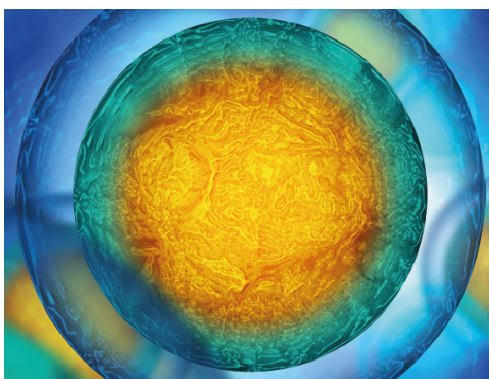


PAPER

An engineered neurovascular unit for modeling neuroinflammation

To cite this article: Suyeong Seo *et al* 2021 *Biofabrication* 13 035039

View the [article online](#) for updates and enhancements.



Biophysical Society

IOP | ebooks™

Your publishing choice in all areas of biophysics research.

Start exploring the collection—download the first chapter of every title for free.

Biofabrication



PAPER

An engineered neurovascular unit for modeling neuroinflammation

RECEIVED
1 December 2020

REVISED
24 March 2021

ACCEPTED FOR PUBLICATION
13 April 2021

PUBLISHED
5 May 2021

Suyeong Seo^{1,2,10}, Chi-Hoon Choi^{3,4,10}, Kyung Sik Yi³, Seung U Kim⁵, Kangwon Lee⁶, Nakwon Choi^{1,7,8,*} , Hong Jun Lee^{4,9,*}, Sang-Hoon Cha^{3,4,*} and Hong Nam Kim^{1,7,*} 

- ¹ Brain Science Institute, Korea Institute of Science and Technology (KIST), Seoul 02792, Republic of Korea
 - ² Program in Nano Science and Technology, Graduate School of Convergence Science and Technology, Seoul National University, Seoul 08826, Republic of Korea
 - ³ Department of Radiology, Chung Buk National University Hospital, Cheongju, Chung Buk, Republic of Korea
 - ⁴ College of Medicine, Chung Buk National University, Cheongju, Chung Buk 28644, Republic of Korea
 - ⁵ Division of Neurology, Department of Medicine, UBC Hospital, University of British Columbia, Vancouver, BC, Canada
 - ⁶ Department of Applied Bioengineering, Graduate School of Convergence Science and Technology, Seoul National University, Seoul 08826, Republic of Korea
 - ⁷ Division of Bio-Medical Science and Technology, KIST School, Korea University of Science and Technology (UST), Seoul 02792, Republic of Korea
 - ⁸ KU-KIST Graduate School of Converging Science and Technology, Korea University, Seoul 02841, Republic of Korea
 - ⁹ Research Institute, eBiogen Inc., Seoul, Republic of Korea
 - ¹⁰ These authors contributed equally to this work
- * Authors to whom any correspondence should be addressed.

E-mail: nakwon.choi@kist.re.kr, leehj71@gmail.com, shcha@chungbuk.ac.kr and hongnam.kim@kist.re.kr

Keywords: neurovascular unit, blood-brain barrier, co-culture, *in vitro* model, vascular permeability, neuroinflammation
Supplementary material for this article is available [online](#)

Abstract

The neurovascular unit (NVU) comprises multiple types of brain cells, including brain endothelial cells, astrocytes, pericytes, neurons, microglia, and oligodendrocytes. Each cell type contributes to the maintenance of the molecular transport barrier and brain tissue homeostasis. Several disorders and diseases of the central nervous system, including neuroinflammation, Alzheimer's disease, stroke, and multiple sclerosis, have been associated with dysfunction of the NVU. As a result, there has been increased demand for the development of NVU *in vitro* models. Here, we present a three-dimensional (3D) immortalized human cell-based NVU model generated by organizing the brain microvasculature in a collagen matrix embedded with six different types of cells that comprise the NVU. By surrounding a perfusable brain endothelium with six types of NVU-composing cells, we demonstrated a significant impact of the 3D co-culture on the maturation of barrier function, which is supported by cytokines secreted from NVU-composing cells. Furthermore, NVU-composing cells alleviated the inflammatory responses induced by lipopolysaccharides. Our human cell-based NVU *in vitro* model could enable elucidation of both physiological and pathological mechanisms in the human brain and evaluation of safety and efficacy in the context of high-content analysis during the process of drug development.

1. Introduction

Cerebral blood vessels have a distinct structure known as the blood-brain barrier (BBB); the BBB is selectively permeable to molecules and inhibits the entry of toxic molecules into the brain [1–4]. Astrocytes and pericytes (PCs) are known to support this unique barrier function and interact with brain endothelial cells (bECs) to maintain and control vascular integrity under physiological and pathological conditions [2, 5–11]. There are several types of transport pathways

for molecules to pass across the BBB [12–15]. For instance, essential nutrients for cell survival, such as glucose and glutamine, are transported into the brain through their specific transport systems, which are controlled by neurons that are the most significant consumers of these nutrients, depending on their metabolic cycle [16–18]. Additionally, when cerebral blood vessels are disrupted, neurotoxic molecules in the blood, including fibrinogen, thrombin, and other enzymes and serum proteins, tend to deposit near the damaged vessels and affect neuronal functions

[19, 20]. As a result, the interaction between brain blood vessels and neurons is critical to understand the pathogenesis of neurodegenerative diseases and neuronal dysfunction [21–25].

From an outward view of brain blood vessels, the neurovascular unit (NVU) lies at a hierarchically high level. The NVU is composed of bECs, astrocytes, PCs, neurons, microglia, and oligodendrocytes, all of which contribute to vascular and neuronal functions as outlined below [26–28] (figure 1(A)).

- (a) Astrocytes and PCs are in direct contact with the endothelial lining and enhance vascular integrity [1, 5–8, 11, 29–31].
- (b) Neurons, away from the BBB, form synapses that transmit signals between neurons and synaptically interact with astrocytes [32–35].
- (c) Microglia are the resident immune cells in the brain and regulate immune responses [36, 37].
- (d) Oligodendrocytes support neuronal metabolism [38–40].

Although the roles of each cell type are reported, the effects of their mutual interactions and the brain microenvironment as a whole have not yet been thoroughly investigated. Therefore, *in vitro* models that can recapitulate cellular functions, cell-to-cell interactions, and the brain microenvironment at the tissue scale are an emerging need [41, 42].

Animal models, while enabling reproduction of the complexity of *in vivo* environments, are expensive and are increasingly associated with critical ethical issues. More importantly, genetic and phenotypic differences between animal models and humans have continuously been reported to increase failure and cause poor predictability in drug screening, as well as in pathological studies in clinical settings [43–45]. Conventional two-dimensional (2D) culture systems such as Transwell® and well plates have the advantage of simplicity for assessing cellular behaviors and drug responses; however, these 2D tools show low levels of barrier function primarily because of the limited culture environment (i.e. cells cultured on 2D rigid plates or membranes) [41, 46, 47]. Therefore, various three-dimensional (3D) and pseudo-3D (i.e. combinations of 2D and 3D settings) NVU *in vitro* models have shown promising potential with regard to reproducing the microphysiological environment in the brain by mimicking the 3D architecture of both the brain vasculature and ECM and employing human-originated cells [28, 48–50]. However, the existing NVU *in vitro* models are limited to co-culture with up to three or four cell types, which do not include perivascular, neuronal, or glial cells [46, 51]. In other words, none of the existing *in vitro* models, to date, have attempted to co-culture all seven aforementioned human-originated cell types to reconstruct the NVU *in vitro*.

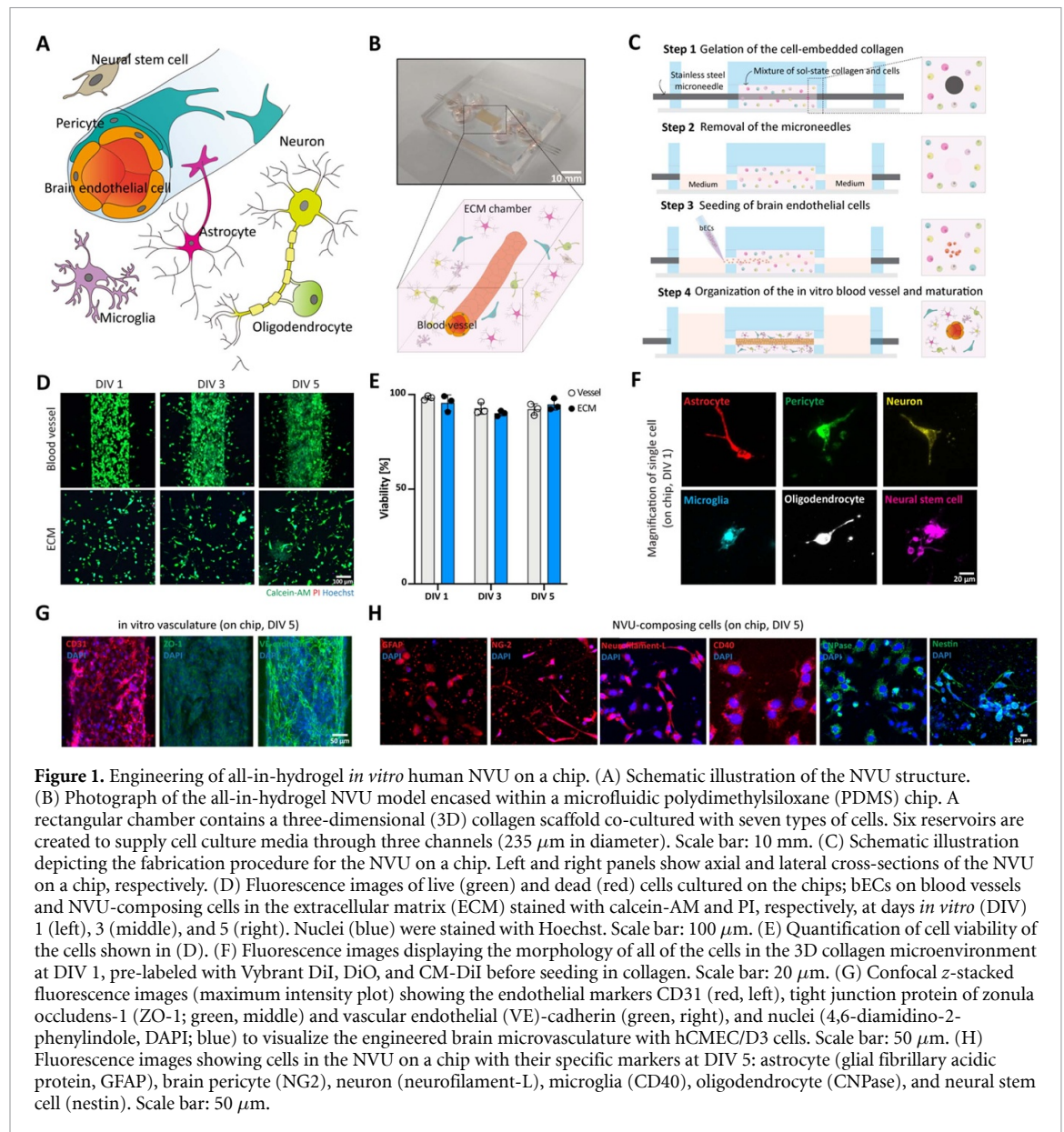
Here, we report a 3D human cell-based NVU model established by co-culturing six types of immortalized cells in a collagen matrix with embedded brain microvasculature. By surrounding a perfusable brain endothelium with six types of NVU-composing cells, we demonstrated a significant impact of the 3D co-culture on the maturation of the barrier function and regulation of an inflammatory response to an exogenous stimulant. Cytokine arrays revealed that the inflammatory response resulted from cellular interactions between the multiple types of NVU-composing cells at a 3D tissue scale. Our human immortalized cell-based NVU *in vitro* model could enable elucidation of both physiological and pathological mechanisms in the human brain and evaluation of safety and efficacy in the context of high-content analysis during the process of drug development.

2. Method

2.1. Fabrication of a microfluidic PDMS chip to house all-in-hydrogel NVU

We used polydimethylsiloxane (PDMS; SYLGARD™ 184 Silicone Elastomer; Dow Corning Inc.) as a housing material to surround cell-laden type I collagen. The microfluidic PDMS chip for housing all-in-hydrogel NVU consisted of three layers: (a) a middle PDMS layer with a central rectangular through-hole connected to three parallel cylindrical microchannels; (b) a top PDMS layer plasma-bonded on the middle layer as a lid to create a central chamber for the collagen scaffold; and (c) a bottom glass slide that was also plasma-bonded with the middle layer (figure S1 (available online at stacks.iop.org/BF/13/035039/mmedia)).

The PDMS base polymer was mixed thoroughly with a curing agent at a weight ratio of 10:1. After degassing in a vacuum chamber to remove microbubbles in the PDMS mixture, it was poured onto a duralumin master in which three stainless steel microneedles (outer diameter: 235 μm ; DASAN Cut) were pre-inserted, for the fabrication of the middle layer. After crosslinking in an oven at 80 °C for at least 3 h, the needles were removed and the PDMS layer were gently separated from the mold. This layer was punched into a rectangular shape (4 × 10 mm) and then bonded to an unpatterned 1 mm thick PDMS layer with oxygen plasma (FEMTO Science). We next used biopsy punches (Miltex) to create six in- and outlet reservoirs (8 mm in diameter) and two collagen injection ports (1 mm in diameter). The three microneedles were inserted through the PDMS microchannels again and bonded to a glass slide (50 × 70 × 0.15 mm; Matsunami) by oxygen plasma treatment. The fabrication process is illustrated in figure S1. To attach the collagen matrix onto the PDMS chamber, we coated the chamber sequentially with 1% (v/v) polyethyleneimine for 30 min



and 0.1% (v/v) glutaraldehyde for 30 min [52, 53]. The surface-coated PDMS chamber was then washed with phosphate-buffered saline (PBS) at least three times to remove unbound molecules that could be cytotoxic, and the chamber was stored at 4 °C until further use.

2.2. Culture of human cell resources composing the NVU

The commercially available human cerebral microvascular endothelial cell line hCMEC/D3 (Cedarlane) was cultured in endothelial cell basal medium-2 (Lonza) supplemented with hydrocortisone, ascorbic acid, vascular endothelial growth factor, long arginine 3-insulin-like growth factor-1, human epidermal growth factor, gentamicin sulfate-amphotericin (GA-1000), human fibroblast growth factor-B, heparin, and 2% (v/v) fetal bovine serum (FBS), according to the manufacturer's protocol, and

maintained in a humidified atmosphere containing 5% CO₂ at 37 °C.

Telencephalon tissue was used to prepare immortalized cell lines, except for bECs, and dissociated to generate brain cells, as previously reported [54–60]. Human neurons (F3.ngn1) [60], human astrocytes (L1.AST) [54], human microglia (HMO6) [59], human oligodendrocytes (F3.olg2) [56], and human neural stem cells (F3) [55, 57, 58] were generated by transfection with *v-myc* and *c-myc* genes of brain cells and maintained under the recommended culture conditions. These cells were obtained from the University of British Columbia. Human pericytes (L1.PC) were generated from human brain vascular PCs (ScienCell).

Human microglia (HMO6), oligodendrocytes (F3.olg2), and neural stem cells (F3) were maintained in Dulbecco's modified Eagle's medium (DMEM) without phenol red (Wegene)

supplemented with 5% (v/v) FBS (GenDEPOT) and 5 $\mu\text{g ml}^{-1}$ gentamicin (Welgene) in a humidified atmosphere with 5% CO_2 at 37 °C. These cells were subcultured every 2–3 d. Human neurons (F3.ngn1) were maintained in Neurobasal-A medium (Gibco) supplemented with 2% (v/v) FBS (GenDEPOT), 5 $\mu\text{g ml}^{-1}$ gentamicin (Welgene), and B-27 plus supplement (Gibco). Human neurons were subcultured every 3–4 d. Human astrocytes (L1.AST) were maintained in astrocyte medium (Gibco) supplemented with 2% (v/v) FBS (GenDEPOT), 5 $\mu\text{g ml}^{-1}$ gentamicin (Welgene), and G5 plus supplement (Gibco). Human astrocytes were subcultured every 3 d. Doxycycline was added to the medium every 2 d at 1 $\mu\text{g ml}^{-1}$ to promote cellular proliferation. Human brain vascular pericytes (L1.PC) were established by transfection with *v-myc*, as described above, and maintained in PC medium (ScienCell) supplemented with 2% (v/v) FBS and PC growth supplement (ScienCell). These cells were subcultured every 4 d. Notably, we added human neural stem cells, which constitute less than 1% of the brain, to help co-culture of other NVU-composing cells while remaining undifferentiated and secreting growth factors.

The immortalized human microglia-SV40 cell line (ABM) was used for a decoupling assay in inflammation. The cells were maintained in DMEM-F12 (D6421; Sigma Aldrich) containing 10% (v/v) FBS (Corning) and 1% (v/v) penicillin streptomycin (Gibco).

To track the morphological changes in NVU-composing cells in collagen, we pre-labeled each cell type with the Vybrant™ Multicolor Cell-Labeling Kit (V22889; Thermo Fisher) before seeding, according to the manufacturer's protocol. First, each cell type was suspended in serum-free medium at a density of 1×10^6 cells ml^{-1} . The labeling reagent (5 μl) was added to 1 ml of the cell suspension, followed by incubation for 20 min at 37 °C. Then, the pre-labeled cell suspension was centrifuged, and the supernatant was rinsed three times with serum-free media to remove any residual labeling reagent. Finally, the pre-labeled cells were mixed with collagen and cultured on our chip, as described below. The morphologies of the cells were monitored using a laser scanning confocal microscope (LSM 700; Zeiss).

2.3. Collagen preparation

To prepare collagen to seed NVU-composing cells, neutralized (pH ~ 7.5 , determined by phenol red in the mixture) collagen solution was prepared as previously described [61]. In brief, commercially available rat tail collagen type I (stock concentration of ~ 10 mg ml^{-1} ; Corning) was diluted to a final concentration of 3 mg ml^{-1} by adding 10 \times DMEM (Sigma-Aldrich), 1 \times DMEM (Welgene), and 0.5 N NaOH (Sigma-Aldrich) according to the manufacturer's instructions. The entire procedure was performed on

ice to prevent undesired initiation of gelation before injection into the PDMS chamber.

2.4. Fabrication of brain endothelial lumen and co-culture of NVU-composing cells in collagen

For the 3D co-culture of NVU-composing cells, except for bECs, cell suspensions containing astrocytes, PCs, neurons, microglia, oligodendrocytes, and neural stem cells were transferred to a sol state of the neutralized collagen solution and mixed gently at a final seeding density of 1×10^5 cells ml^{-1} . Thereafter, the cell-seeded collagen was injected into the rectangular PDMS chamber ($4 \times 10 \times 1$ mm), where the three microneedles (wall-to-wall inter-channel distance of 1 mm) were pre-inserted. The NVU chip was incubated at 37 °C for 30 min for collagen gelation, and the microneedles were subsequently removed from the gelled scaffold. As a result, hollow and cylindrical lumen channels (235 μm in diameter) was formed in the middle of the collagen scaffold. After incubating the chip with culture media applied to reservoirs for at least 1 h in an incubator, bECs (hCMEC/D3; 4×10^6 cell ml^{-1}) were delivered through the central microchannel and allowed to attach to the luminal surface of the collagen channel. The chip was flipped for 10 min after the introduction of the bEC cell suspension to allow uniform cell seeding on the cylindrical surface. Finally, culture media was infused through the bEC-plated channel to wash out unattached cells. The NVU chip was maintained in a humidified atmosphere with 5% CO_2 at 37 °C, and the medium was changed every day.

2.5. Estimation of cell viability

The bECs and NVU-composing cells cultured on chips were stained with calcein-AM (C1430; ThermoFisher), propidium iodide (PI; P4564; Sigma-Aldrich), and Hoechst 33342 (H3570; Invitrogen) at DIV 1, 3, and 5. A staining solution was prepared by mixing each reagent with serum-free media to a working concentration of 1 μM for calcein-AM, 1 $\mu\text{g ml}^{-1}$ PI, and 10 $\mu\text{g ml}^{-1}$ Hoechst 33342. The cells in the chips were incubated with the staining solutions at 37 °C for 30 min and then washed with cell culture media before fluorescence imaging. To quantify cell viability, we counted individual green (live) and red (dead) cells from images acquired from multiple chips ($n = 3$) and calculated the ratio of green to red cells for blue (total) cells.

2.6. Immunofluorescence staining

After culturing the NVU chips for 5 d, we fixed the cells with 4% (v/v) paraformaldehyde for 30 min and then permeabilized them with a solution containing 0.3% (v/v) Triton X-100 and 3% (w/v) bovine serum albumin (BSA) for 30 min by delivering the reagents through the three microchannels. As primary antibodies, rabbit anti-CD31 antibody (ab32457; Abcam), mouse anti-vascular endothelial

(VE)-cadherin antibody (SC-9989; SantaCruz), mouse anti-zonula occludens-1 (ZO-1) antibody (33–9100; Invitrogen), mouse anti-intercellular adhesion molecule 1 antibody (MA133754; Invitrogen), rabbit anti-glial fibrillary acidic protein (GFAP) antibody (Z0334; Dako), rabbit anti-neural/glial antigen 2 (NG2) antibody (AB5320; Millipore), rabbit anti-CD40 antibody (ab58391; Abcam), anti-CD11b antibody (NB110-89474; Novus Biologicals), rabbit anti-neurofilament L antibody (AB9568; Millipore), mouse anti-CNPase antibody (MAB326; Millipore), and mouse anti-nestin antibody (MAB5326; Millipore) were diluted (1:200) with 3% [w/v] BSA and then kept with the chips for 4 h at room temperature. After washing the microchannels with PBS, the NVU chips were incubated with secondary antibodies, including Alexa 488-labeled anti-mouse (A11001; dilution factor of 1:200; ThermoFisher), Alexa 594-labeled anti-rabbit (A110123; dilution factor of 1:200; ThermoFisher), and Alexa 488-labeled anti-rabbit (ab150077; dilution factor of 1:200; Abcam) antibodies for 2 h at room temperature. For nuclei staining, 4,6-diamidino-2-phenylindole solution was diluted (1:1000) and incubated with the cells for 30 min at room temperature. For immunostaining of the cytoskeleton, the cells were incubated with phalloidin-TRITC (P1951, Sigma-Aldrich) diluted with 1% (v/v) DMSO solution as per the recommended protocol. Fluorescence *z*-stack images were acquired using a laser scanning confocal microscope (LSM 700; Zeiss).

2.7. Quantitative estimation of barrier function (transendothelial permeability) in the NVU chips

We assessed barrier function by measuring the transendothelial permeability of our engineered endothelium, as previously described [62]. In brief, culture media was aspirated from each reservoir, and then 10 μM of 4 kDa and 40 kDa fluorescein isothiocyanate (FITC)-dextran (Sigma-Aldrich) in PBS was added to the brain-vascularized microchannel. Immediately after the delivery of FITC-dextran, molecular transport (i.e. diffusion across the brain endothelium toward the surrounding tissue) was monitored by sequential acquisition of confocal fluorescence images (LSM 700; Zeiss) for 5 min at 1 min intervals. Our custom MATLAB (Mathworks) code allowed the quantification of transendothelial permeability by analyzing temporal evolutions of fluorescence intensity in the perivascular space of a cylindrical coordinate.

2.8. Inflammation assay

To induce an inflammatory condition and determine the protective effect of NVU, lipopolysaccharide (LPS; Sigma-Aldrich), a known factor in inflammation-associated diseases, was used. The mature endothelium was incubated with a final concentration of 100 $\mu\text{g ml}^{-1}$ LPS in culture media for 1 d, followed by washing with fresh medium to

remove residual LPS. Then, 40 kDa FITC-dextran was infused into the vessel, and fluorescence images were acquired to quantify transendothelial permeability, as described above.

2.9. Cytokine microarray

To detect cytokines secreted by cells in our NVU chips, we collected conditioned culture media from the reservoirs. Following the service provider's protocol, the collected media was purified and analyzed to detect 1000 human cytokines using a human L1000 microarray (e-biogen Inc.).

2.10. Statistical analysis

All quantitative data are expressed as mean \pm standard error of the mean values. Statistical analysis was performed using a one-way analysis of variance (ANOVA) on Prism (GraphPad). For the determination of statistical significance, *p*-values < 0.05 were considered to be significant.

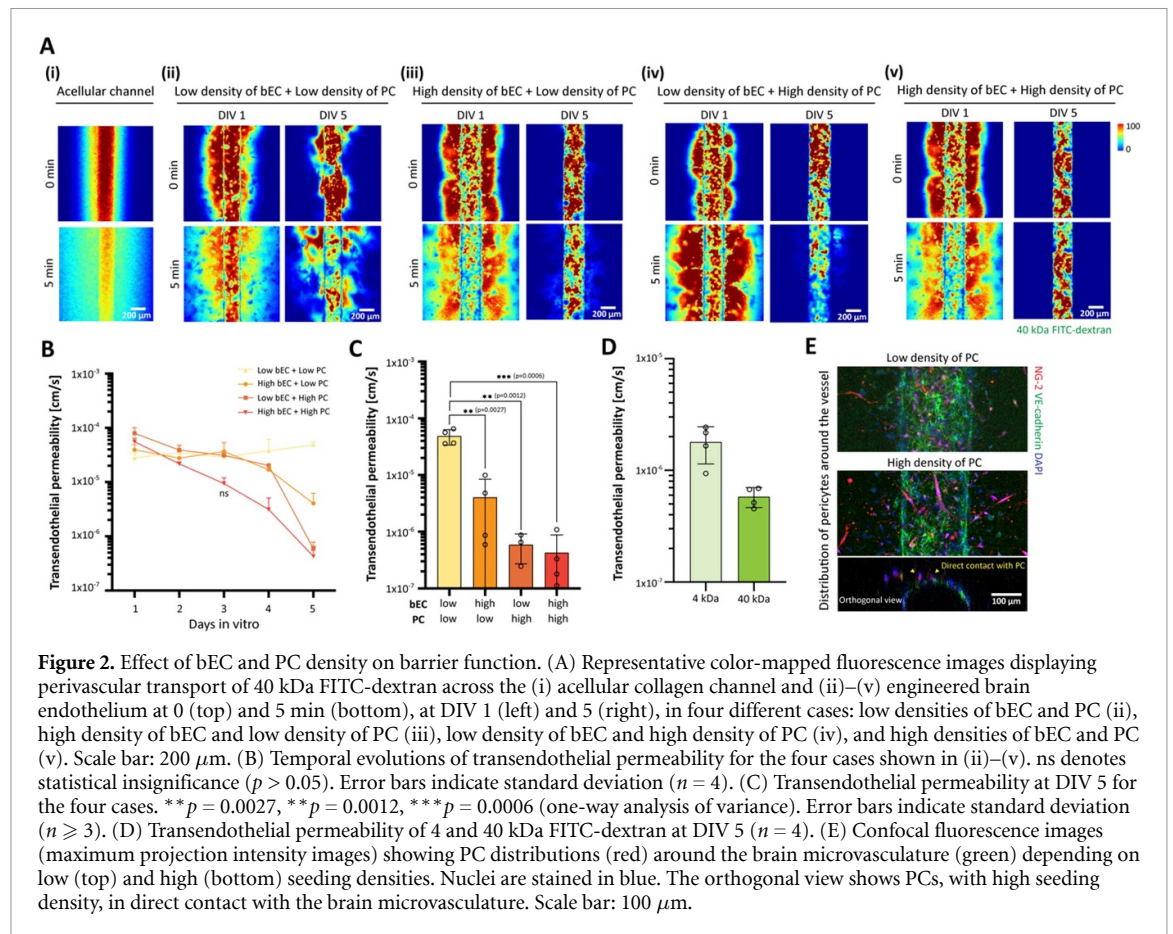
3. Results

3.1. Engineered *in vitro* microfluidic model for recapitulating NVU

Our NVU model consisted of a perfusable cylindrical brain endothelium embedded in collagen where six types of NVU-composing cells resided. To engineer the lumen structure *in vitro*, we exploited microneedles with a diameter of 235 μm as templates for microfluidic endothelialization (figure 1(C)), as reported previously [62]. After gelation of the collagen scaffold, gentle removal of the microneedles allowed the formation of microchannels with identical sizes and shapes.

We used the hCMEC/D3 cell line to reconstruct the human cerebral microvasculature. To ensure attachment of human BECs uniformly on the luminal surface of the collagen microchannels, we flipped our NVU chip once 10 min after introducing the BEC suspension. The attached BECs covered the entire surface of the collagen microchannel and were organized into a monolayer of 3D straight, cylindrical brain endothelium within 2–3 d. As BECs tend to invade the soft matrix after organization into the monolayer due to their high proliferative property, these cells were cultured on the stiffer collagen channel to facilitate visualization of junctional markers. We verified the formation of cerebral microvasculature *in vitro* by the assessing the expression of endothelial cell-specific markers such as CD31, ZO-1, and VE-cadherin (figure 1(G)).

We chose 3 mg ml^{-1} (0.3% (w/v)) of collagen type I as the scaffold material primarily to maintain the structural fidelity of the microfluidic endothelium while matching the softness [62–64] and viscoelasticity [65] of neural tissues. The choice of a suitable range of mechanical properties is crucial as the surrounding matrix also contains many living adherent



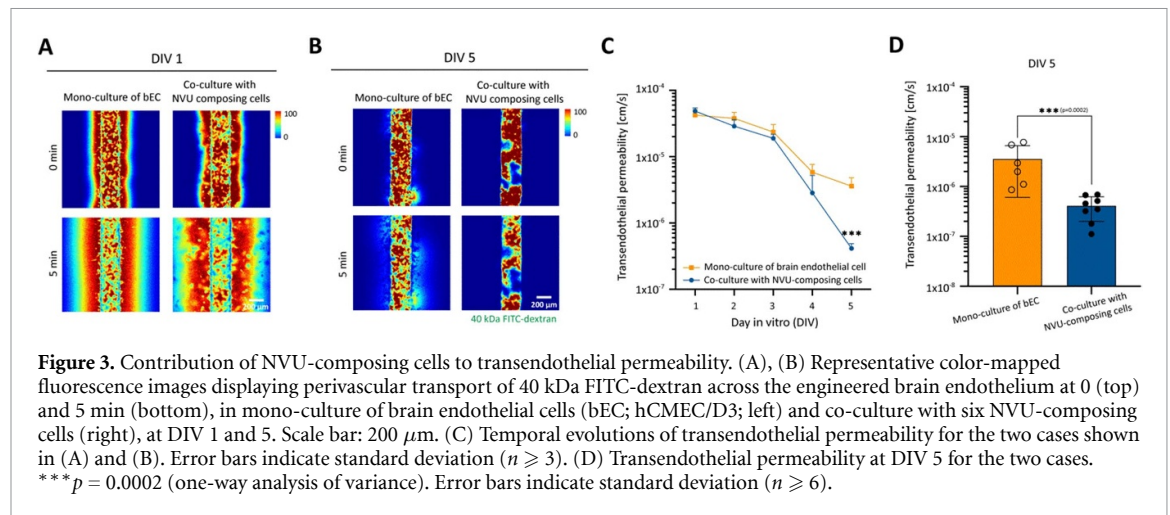
cells capable of pulling the matrix. We seeded astrocytes, PCs, neurons, microglia, oligodendrocytes, and neural stem cells in 3 mg ml^{-1} collagen before gelation. We tracked the morphological changes of individual cell types with cell-labeling agents and confirmed that all six cell types had spread well in the 3D hydrogel (figure 1(F)). Additionally, we estimated the viability of bECs and NVU-composing cells cultured in the chips. We confirmed that all the cells remained viable, with no abnormal cell death, throughout the culture period (i.e. DIV 1, 3, and 5), and with viability higher than 90% (figures 1(D) and (E)). These data indicate that our fabricated NVU on a chip and on-chip microenvironment were suitable for 3D co-culture. Immunocytochemistry confirmed that these NVU-composing cells expressed cell type representative markers: astrocyte-GFAP, pericyte-NG2, neuron-neurofilament L, microglia-CD40, oligodendrocyte-CNPase, and neural stem cell-*nestin* (figure 1(H)).

3.2. Density of brain PCs as a pivotal parameter for the barrier function of NVU

Cerebral blood vessels in the NVU have distinct barriers known as the BBB that regulates the molecular transport at the interface between the vascular system and the brain tissue. Tight junctions (TJs) formed between adjacent endothelial cells physically inhibit the entry of molecules and protect brain

tissue from potentially toxic substances. Therefore, an engineered NVU model should be capable of mimicking this barrier function. To evaluate barrier function, we measured the transendothelial permeability of a fluorescent model molecule, FITC-dextran, by scanning the temporal evolution of molecular transport from the brain microvasculature to the surrounding collagen space. More specifically, immediately after loading $10 \mu\text{M}$ of 4 kDa (Stoke's radius of $\sim 1.4 \text{ nm}$) and 40 kDa FITC-dextran (Stoke's radius of $\sim 4.5 \text{ nm}$) into the engineered 3D brain endothelium, we acquired a series of confocal fluorescence micrographs. We then analyzed fluorescence in the perivascular region using a custom MATLAB code, as previously described [62]. This technique allowed for quantitative estimation of transendothelial permeability.

Based on our assessment, we found that the seeding density of human bECs and PCs was critical for low permeability levels within a week. First, we controlled the density of bECs while keeping that of PCs and other cell types identical. When we loaded the collagen microchannel with $4 \times 10^6 \text{ cell ml}^{-1}$ (a high density) (figure 2(A) (iii)), transendothelial permeability reached $4.04 \times 10^{-6} \pm 4.36 \times 10^{-6} \text{ cm s}^{-1}$ at DIV 5, whereas $3 \times 10^6 \text{ cell ml}^{-1}$ (a low density) (figure 2(A) (ii)) led to higher mean permeability of $4.86 \times 10^{-5} \pm 1.47 \times 10^{-5} \text{ cm s}^{-1}$ at DIV 5 (figures 2(B) and (C)). We also controlled



the seeding density of PCs because brain PCs have been reported to be the primary regulators of vascular integrity and barrier function [8]. We found that increasing the density of PCs from 3.25×10^3 to 3×10^4 cell ml^{-1} (i.e. 30% of the total cell population in the collagen scaffold) reduced transendothelial permeability (figure 2(A) (iii) and (v)) significantly to $4.28 \times 10^{-7} \pm 4.5 \times 10^{-7}$ cm s^{-1} at DIV 5 (figures 2(B) and (C)). Interestingly, the density of bECs, combined with the high density of PCs, affected the maturation of vascular permeability early, starting from DIV 3 (figure 2(B)). At DIV 5, the matured brain endothelium showed low transendothelial permeability ($P_{4 \text{ kDa}} = 1.8 \times 10^{-6} \pm 0.66 \times 10^{-6}$ cm s^{-1} and $P_{40 \text{ kDa}} = 5.84 \times 10^{-7} \pm 1.18 \times 10^{-7}$ cm s^{-1}) (figure 2(D)).

These data suggest that the high seeding density of PCs allowed for acquisition of the enhanced barrier functionality. Additionally, we observed many more PCs near the brain microvasculature and some were in direct contact with the microfluidic brain endothelium (figure 2(E)). These observations suggest that the enhanced barrier function could be attributed to enhanced interactions between bECs and PCs via direct contact and paracrine effects. However, we noted that direct contact did not result from active migration of PCs toward the brain microvasculature within 5 d of culture. In another study, such active migration of PCs to microfluidic endothelia formed with HUVECs occurred in approximately 2 weeks [52].

3.3. NVU-composing cells supporting the maturation of the transport barrier in a cytokine-mediated manner

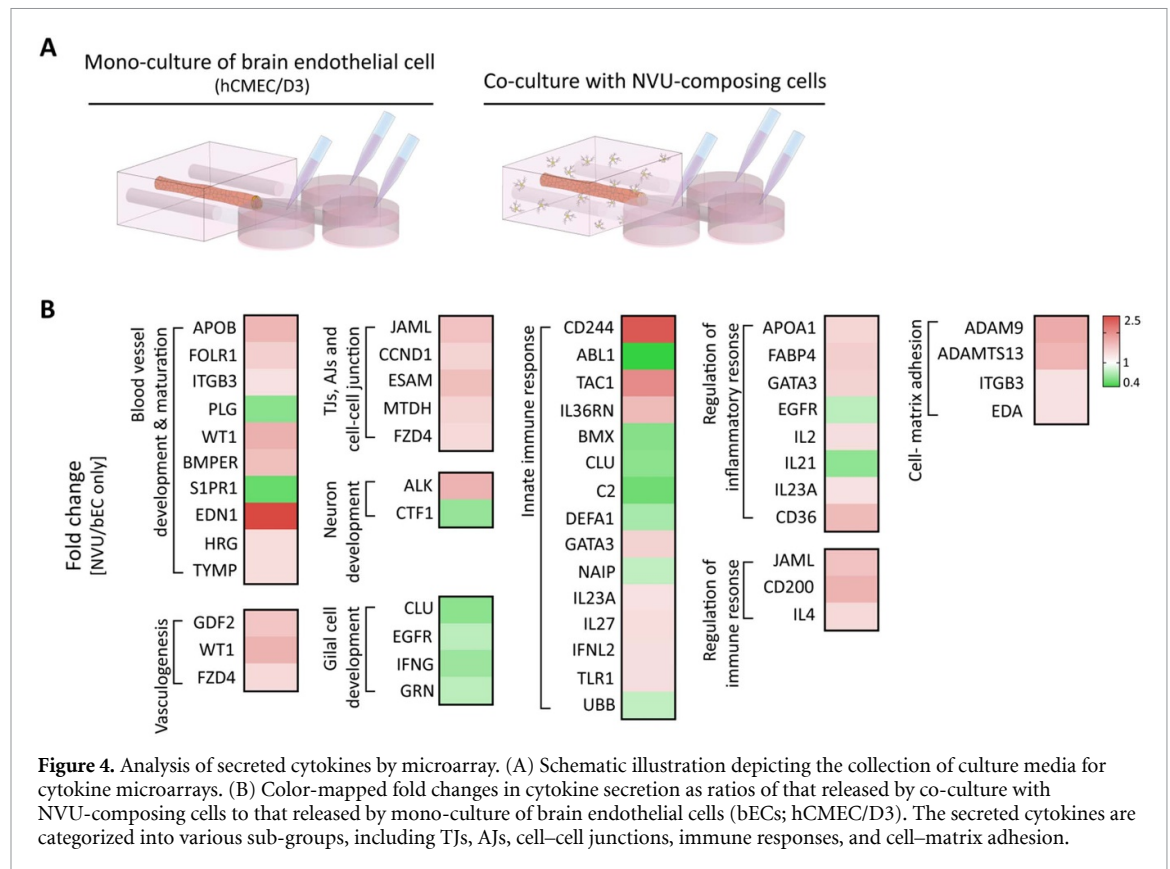
We next confirmed whether the co-culture of multiple types of NVU-composing cells affects the NVU barrier function. When comparing the mono-culture of bECs and the co-culture of six types of NVU-composing cells along with bECs, the co-culture showed a tighter barrier with low transendothelial permeability of 2.96

$\times 10^{-7} \pm 2.12 \times 10^{-7}$ cm s^{-1} at DIV 5 than did the mono-culture ($P_{\text{mono}} = 5.05 \times 10^{-6} \pm 2.49 \times 10^{-6}$ cm s^{-1}) (figure 3(D)). These results indicate that NVU-composing cells support the maturation of the transport barrier.

To determine whether soluble factors secreted by NVU-composing cells may induce maturation of the vascular barrier function, we analyzed cytokine levels. We collected cell culture media from our NVU chip at DIV 5 and performed cytokine microarray analysis (figure 4(A)). When quantifying relative differences in cytokine secretion as ratios of that secreted by the co-culture of NVU-composing cells and bEC to that secreted by monoculture of bECs, some significant differences were observed in several categories. Notably, large amounts of cytokines associated with blood vessel development and maturation and vasculogenesis-related cytokines increased in the co-culture (i.e. the NVU chip) (figure 4(B)). Furthermore, the increased level of factors related to cell-to-cell junctions, such as TJs and adherens junctions (AJs) supported the result of the lower transendothelial permeability observed in the NVU chip. These results suggest a paracrine effect by soluble factors released in the multicellular microenvironment, which would be essential for recapitulating the *in vivo* physiological structure and functionality. Interestingly, the cytokines associated with immune and inflammatory regulation also increased, which could be attributed to co-culturing with microglia. We have described the effects of the increased cytokines related to immune and inflammatory regulation in more detail in the following section.

3.4. NVU-composing cells alleviating LPS-induced neuroinflammation

Among NVU-composing cells, astrocytes and microglia are known to play a regulatory role in both the barrier function and the immune response within the central nervous system [6, 37, 66]. To confirm the inflammation modulation capability

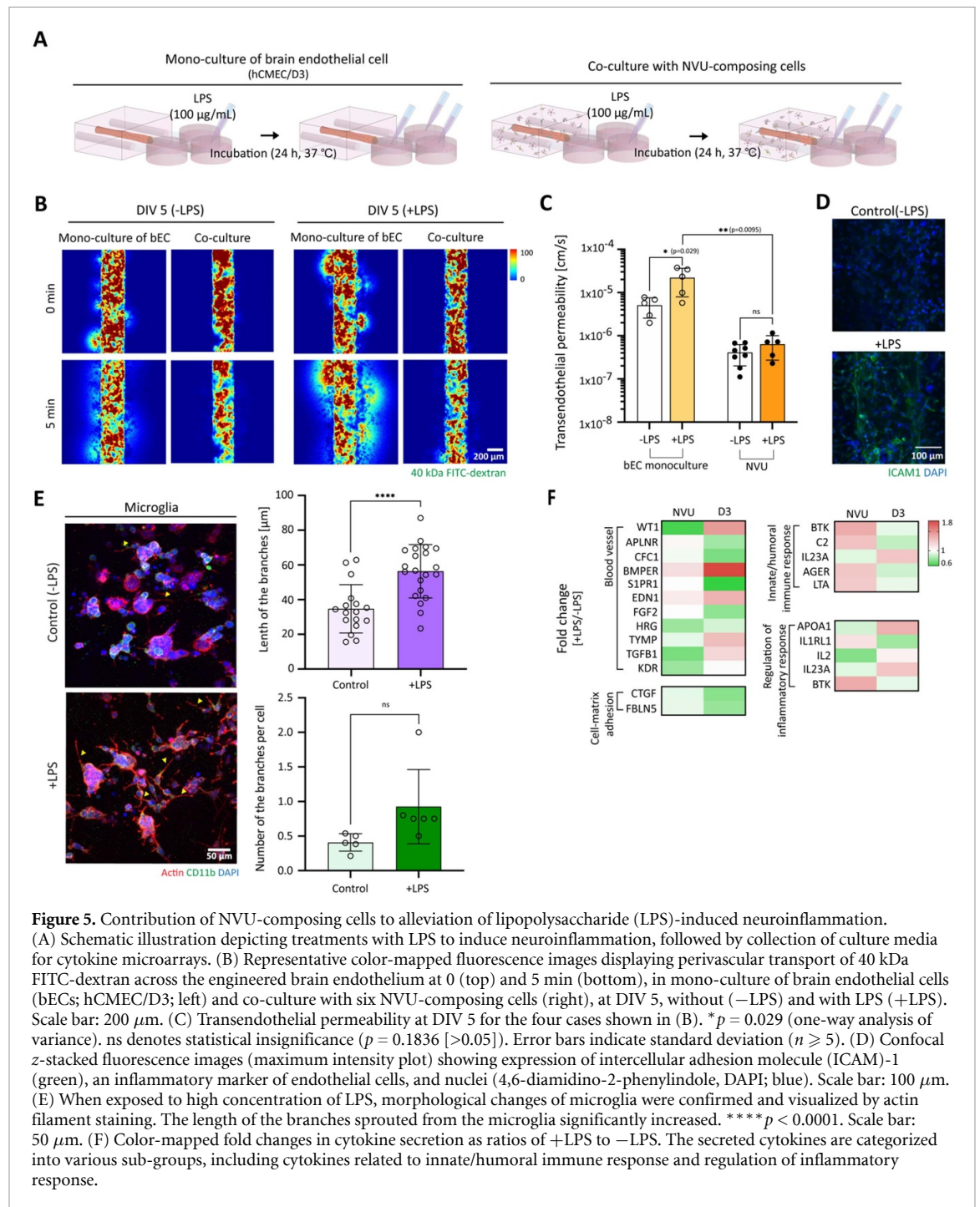


of NVU-composing cells, we induced inflammation by delivering an LPS solution ($100 \mu\text{g ml}^{-1}$) through the engineered 3D brain endothelium at DIV 5 and incubating for 24 h (figure 5(A)). Given that we introduced the stimulant through the blood vessel, not through the brain tissue region, this approach could partly mimic vasculature-originated inflammation. As shown in figures 5(B) and (C), the leakage of 40 kDa FITC-dextran increased upon LPS exposure only in the bEC mono-culture. In contrast, no significant change in vascular permeability occurred in the NVU models (figure 5(C)), although bECs expressed the inflammatory marker ICAM-1 (figure 5(D)). Additionally, we decoupled microglia from other NVU-composing cells to separately monitor the response of brain immune cells during inflammation. Morphological modifications of microglia were observed and visualized by phalloidin staining. As shown in figure 5(E), inflammation-stimulated microglia had elongated branches with a similar number of branches in the normal state. This morphological change is in agreement with that reported in a previous study that used an immortalized microglial cell line [67]. These results suggest that NVU-composing cells respond to inflammatory stimuli and modulate the barrier function under inflammatory conditions to maintain their normal function. We also measured changes in the cytokine secretion before and after the LPS treatment, and microarray data displayed fold changes as ratios of '+LPS' to '-LPS' (figure 5(F)). According to the

analysis, the cytokines associated with blood vessels, immune response, and inflammatory response showed marked changes after LPS-induced stimulation. Notably, in the mono-culture of bECs, the secretion of bone morphogenic protein-binding endothelial regulator (BMPER), which is known to activate endothelial sprouting and weaken the adhesion between cells and the matrix, increased when LPS stimulated the brain microvasculature. This cytokine pattern indicates that an inflammatory material can easily damage the cell–cell and cell–matrix integrity and loosen the barrier function in bEC mono-culture models. In addition, level of Bruton's tyrosine kinase, which regulates the production of mediators of inflammation, was increased in our NVU model. This upregulation represents an enhanced inflammatory defense system in a multicellular microenvironment under external stimulation.

4. Discussion

The NVU, a structural and functional unit in the brain, strictly controls the molecular transport between the brain and cerebral vessels to maintain cerebral homeostasis. Many brain disorders, including dementia, traumatic brain injury, edema, and neuroinflammation, are accompanied by cerebrovascular dysfunction, which is affected by multicellular crosstalk in pathological processes. In recent studies, NVU *in vitro* models have been developed to



mimic the *in vivo* brain microenvironment and function [28, 48–50]. We have also established an all-in-hydrogel NVU *in vitro* model with 3D co-culture and demonstrated the role of NVU-composing cells in the functionality of the NVU.

We used collagen type I, which presents proper softness for mimicking the ECM, as it enables the fabrication of hollow vascular channels and maintenance of structural fidelity without disruption or shrinkage over weeks. In this study, we focused on demonstrating the capability of co-culturing human cerebral endothelial cells on the luminal surface of a cylindrical collagen microchannel and six types of

brain-constituting cells (i.e. PCs, astrocytes, neurons, microglia, oligodendrocytes, and neural stem cells) within the 3D collagen scaffold. As PCs, which serve as a vital component of the BBB, are essential for stabilizing cerebral blood vessels, we controlled the density of PCs in the collagen as a primary microenvironmental factor. When we cultured bECs surrounded by a high density (3×10^4 cell ml^{-1}) of PCs, the brain microvasculature showed a tight barrier function with low permeability. Additionally, to determine whether this vascular functionality was mediated by indirect interactions with some soluble factors secreted from multiple cell types, we analyzed the

cytokine levels in the co-culture media. We found an increased secretion of cytokines related to blood vessel development/maturation and vasculogenesis, such as endothelin 1, Wilms Tumor 1, apolipoprotein B, endothelial cell adhesion molecule, growth differentiation factor 2, junction adhesion molecule like, and BMPER, all of which showed more than 1.5-fold increases in the NVU chip. These data suggest that a paracrine effect of cytokines in the multicellular environment is indispensable for recapitulating *in vivo* functionality.

Inflammation is a hallmark of brain pathogenesis. Physiologically, microglia and astrocytes are known to release various types of molecules to modulate an acute or chronic inflammatory response [66, 68]. To validate the inflammation-regulatory function of our NVU-chip, we exposed the NVU to LPS, a model inflammation stimulant, via the brain endothelium for a day. Interestingly, the disruption of the enhanced barrier function by LPS exposure was significantly less in our NVU model, compared with that in the mono-culture of bECs. Furthermore, when LPS stimulates the brain endothelium, dramatic variations in cytokine secretion are mainly associated with endothelial cell activation. In the co-culture or LPS-stimulated states, high levels of cytokines related to the regulation of immune and inflammatory responses were confirmed in the co-cultured NVU system. These results suggest an enhanced protective effect in the NVU microenvironment, mediated by cytokines from co-cultured cells.

5. Conclusions

We engineered an NVU *in vitro* model by co-culturing six types of NVU-composing cells, including PCs, astrocytes, neurons, microglia, oligodendrocytes, and neural stem cells with a perfusable brain endothelium in a 3D collagen microenvironment. We found that (a) NVU-composing cells, especially brain PCs, are important for the maturation of barrier function, (b) NVU-composing cells alleviate the exogenous stimulant-induced inflammation, and (c) the maturation of barrier function and modulation of inflammatory response are partly regulated in a cytokine-mediated manner. These results consistently support the need for introducing multiple cell types in the fabrication of artificial brain tissue models. Our biomimetic NVU *in vitro* model could serve as a platform for investigating the functions of NVU-composing cells under physiological and pathological conditions and for evaluating the efficacy of drugs with an add-on disease module such as glioblastoma multiforme.

Data availability statement

All data that support the findings of this study are included within the article (and any supplementary files).

Acknowledgments

This research was supported by the Technology Innovation Program (Grant No. 10067787) funded by the Ministry of Trade, Industry & Energy (MOTIE, Korea).

Conflict of interests

The authors declare that there is no conflict of interest.

ORCID iDs

Nakwon Choi  <https://orcid.org/0000-0003-2993-9233>

Hong Nam Kim  <https://orcid.org/0000-0002-0329-0029>

References

- [1] Abbott N J, Patabendige A A, Dolman D E, Yusof S R and Begley D J 2010 Structure and function of the blood–brain barrier *Neurobiol. Dis.* **37** 13–25
- [2] Ballabh P, Braun A and Nedergaard M 2004 The blood–brain barrier: an overview: structure, regulation, and clinical implications *Neurobiol. Dis.* **16** 1–13
- [3] Serlin Y, Shelef I, Knyazer B and Friedman A 2015 Anatomy and physiology of the blood–brain barrier *Seminars in Cell & Developmental Biology* (Amsterdam: Elsevier) pp 2–6
- [4] Weiss N, Miller F, Cazaubon S and Couraud P-O 2009 The blood–brain barrier in brain homeostasis and neurological diseases *Biochim. Biophys. Acta, Biomembr.* **1788** 842–57
- [5] Abbott N J 2002 Astrocyte–endothelial interactions and blood–brain barrier permeability *J. Anat.* **200** 629–38
- [6] Abbott N J, Rönnbäck L and Hansson E 2006 Astrocyte–endothelial interactions at the blood–brain barrier *Nat. Rev. Neurosci.* **7** 41
- [7] Alvarez J I, Katayama T and Prat A 2013 Glial influence on the blood brain barrier *Glia* **61** 1939–58
- [8] Armulik A, Genové G, Mäe M, Nisancioglu M H, Wallgard E, Niaudet C, He L, Norlin J, Lindblom P and Strittmatter K 2010 Pericytes regulate the blood–brain barrier *Nature* **468** 557
- [9] Daneman R, Zhou L, Kebede A A and Barres B A 2010 Pericytes are required for blood–brain barrier integrity during embryogenesis *Nature* **468** 562
- [10] Janzer R C and Raff M C 1987 Astrocytes induce blood–brain barrier properties in endothelial cells *Nature* **325** 253
- [11] Yao Y, Chen Z-L, Norris E H and Strickland S 2014 Astrocytic laminin regulates pericyte differentiation and maintains blood brain barrier integrity *Nat. Commun.* **5** 3413
- [12] Barar J, Rafi M A, Pourseif M M and Omid Y 2016 Blood–brain barrier transport machineries and targeted therapy of brain diseases *BioImpacts* **6** 225

- [13] Jones A R and Shusta E V 2007 Blood–brain barrier transport of therapeutics via receptor–mediation *Pharm. Res.* **24** 1759–71
- [14] Lalatsa A and Butt A M 2018 *Nanotechnology-Based Targeted Drug Delivery Systems for Brain Tumors* (Amsterdam: Elsevier) pp 49–74
- [15] Nicholson C 2001 Diffusion and related transport mechanisms in brain tissue *Rep. Prog. Phys.* **64** 815
- [16] McAllister M S, Krizanac-Bengez L, Macchia F, Naftalin R J, Pedley K C, Mayberg M R, Marroni M, Leaman S, Stanness K A and Janigro D 2001 Mechanisms of glucose transport at the blood–brain barrier: an *in vitro* study *Brain Res.* **904** 20–30
- [17] Patching S G 2017 Glucose transporters at the blood–brain barrier: function, regulation and gateways for drug delivery *Mol. Neurobiol.* **54** 1046–77
- [18] Shah K, DeSilva S and Abbruscato T 2012 The role of glucose transporters in brain disease: diabetes and Alzheimer's disease *Int. J. Mol. Sci.* **13** 12629–55
- [19] Zlokovic B V 2008 The blood–brain barrier in health and chronic neurodegenerative disorders *Neuron* **57** 178–201
- [20] Sweeney M D, Ayyadurai S and Zlokovic B V 2016 Pericytes of the neurovascular unit: key functions and signaling pathways *Nat. Neurosci.* **19** 771–83
- [21] Erickson M A and Banks W A 2013 Blood–brain barrier dysfunction as a cause and consequence of Alzheimer's disease *J. Cerebral Blood Flow Metab.* **33** 1500–13
- [22] Girouard H and Iadecola C 2006 Neurovascular coupling in the normal brain and in hypertension, stroke, and Alzheimer disease *J. Appl. Physiol.* **100** 328–35
- [23] Sweeney M D, Sagare A P and Zlokovic B V 2018 Blood–brain barrier breakdown in Alzheimer disease and other neurodegenerative disorders *Nat. Rev. Neurol.* **14** 133
- [24] Yang Y and Rosenberg G A 2011 Blood–brain barrier breakdown in acute and chronic cerebrovascular disease *Stroke* **42** 3323–8
- [25] Zlokovic B V 2011 Neurovascular pathways to neurodegeneration in Alzheimer's disease and other disorders *Nat. Rev. Neurosci.* **12** 723
- [26] Bosworth A M, Faley S L, Bellan L M and Lippmann E S 2018 Modeling neurovascular disorders and therapeutic outcomes with human-induced pluripotent stem cells *Front. Bioeng. Biotechnol.* **5** 87
- [27] Lippmann E S, Al-Ahmad A, Palecek S P and Shusta E V 2013 Modeling the blood–brain barrier using stem cell sources *Fluids Barriers CNS* **10** 2
- [28] Adriani G, Ma D, Pavesi A, Kamm R D and Goh E L 2017 A 3D neurovascular microfluidic model consisting of neurons, astrocytes and cerebral endothelial cells as a blood–brain barrier *Lab Chip* **17** 448–59
- [29] Arthur F E, Shivers R R and Bowman P D 1987 Astrocyte-mediated induction of tight junctions in brain capillary endothelium: an efficient *in vitro* model *Dev. Brain Res.* **36** 155–9
- [30] Hori S, Ohtsuki S, Hosoya K, Nakashima E and Terasaki T 2004 A pericyte-derived angiopoietin-1 multimeric complex induces occludin gene expression in brain capillary endothelial cells through Tie-2 activation *in vitro* *J. Neurochem.* **89** 503–13
- [31] Thanabalasundaram G, Schneidewind J, Pieper C and Galla H-J 2011 The impact of pericytes on the blood–brain barrier integrity depends critically on the pericyte differentiation stage *Int. J. Biochem. Cell Biol.* **43** 1284–93
- [32] Perea G, Sur M and Araque A 2014 Neuron–glia networks: integral gear of brain function *Front. Cell Neurosci.* **8** 378
- [33] Fields R D and Stevens–Graham B 2002 New insights into neuron–glia communication *Science* **298** 556–62
- [34] Levitan I B and Kaczmarek L K 2015 *The Neuron: Cell and Molecular Biology* (Oxford: Oxford University Press)
- [35] Nicholls J G, Martin A R, Wallace B G and Fuchs P A 2001 *From Neuron to Brain* vol 271 (Sunderland, MA: Sinauer Associates)
- [36] Aloisi F 2001 Immune function of microglia *Glia* **36** 165–79
- [37] Lenz K M and Nelson L H 2018 Microglia and beyond: innate immune cells as regulators of brain development and behavioral function *Front. Immunol.* **9** 698
- [38] Pfeiffer S E, Warrington A E and Bansal R 1993 The oligodendrocyte and its many cellular processes *Trends Cell Biol.* **3** 191–7
- [39] Seo J H, Maki T, Maeda M, Miyamoto N, Liang A C, Hayakawa K, Pham L-D-D, Suwa F, Taguchi A and Matsuyama T 2014 Oligodendrocyte precursor cells support blood–brain barrier integrity via TGF- β signaling *PLoS One* **9** e103174
- [40] Simons M and Trajkovic K 2006 Neuron–glia communication in the control of oligodendrocyte function and myelin biogenesis *J. Cell. Sci.* **119** 4381–9
- [41] Wilhelm I, Fazakas C and Krizbai I A 2011 *In vitro* models of the blood–brain barrier *Acta Neurobiol. Exp.* **71** 113–28
- [42] Wolff A, Antfolk M, Brodin B and Tenje M 2015 *In vitro* blood–brain barrier models—an overview of established models and new microfluidic approaches *J. Pharm. Sci.* **104** 2727–46
- [43] Festing S and Wilkinson R 2007 The ethics of animal research: talking point on the use of animals in scientific research *EMBO Rep.* **8** 526–30
- [44] Hartung T 2008 Thoughts on limitations of animal models *Parkinsonism Relat. Disorders* **14** S81–3
- [45] Potashkin J, Blume S and Runkle N 2011 Limitations of animal models of Parkinson's disease *Parkinson's Dis.* **2011** 658083
- [46] Seo S, Kim H, Sung J H, Choi N, Lee K and Kim H N 2019 Microphysiological systems for recapitulating physiology and function of blood–brain barrier *Biomaterials* **232** 119732
- [47] Naik P and Cucullo L 2012 *In vitro* blood–brain barrier models: current and perspective technologies *J. Pharm. Sci.* **101** 1337–54
- [48] Brown J A, Pensabene V, Markov D A, Allwardt V, Neely M D, Shi M, Britt C M, Hoilett O S, Yang Q and Brewer B M 2015 Recreating blood–brain barrier physiology and structure on chip: a novel neurovascular microfluidic bioreactor *Biomicrofluidics* **9** 054124
- [49] Maoz B M, Herland A, FitzGerald E A, Grevesse T, Vidoudez C, Pacheco A R, Sheehy S P, Park T-E, Dauth S and Mannix R 2018 A linked organ-on-chip model of the human neurovascular unit reveals the metabolic coupling of endothelial and neuronal cells *Nat. Biotechnol.* **36** 865–74
- [50] Bhalerao A, Sivandzade F, Archie S R, Chowdhury E A, Noorani B and Cucullo L 2020 *In vitro* modeling of the neurovascular unit: advances in the field *Fluids Barriers CNS* **17** 1–20
- [51] Alcendor D J, Block III F E, Cliffler D E, Daniels J S, Ellacott K L, Goodwin C R, Hofmeister L H, Li D, Markov D A and May J C 2013 Neurovascular unit on a chip: implications for translational applications *Stem. Cell Res. Ther.* **4** S18
- [52] Zheng Y, Chen J, Craven M, Choi N W, Totorica S, Diaz-Santana A, Kermani P, Hempstead B, Fischbach-Teschl C and López J A 2012 *In vitro* microvessels for the study of angiogenesis and thrombosis *Proc. Natl Acad. Sci.* **109** 9342–7
- [53] Morgan J P, Delnero P F, Zheng Y, Verbridge S S, Chen J, Craven M, Choi N W, Diaz-Santana A, Kermani P and Hempstead B 2013 Formation of microvascular networks *in vitro* *Nat. Protocols* **8** 1820–36
- [54] Choi S S, Lee H J, Lim I, Satoh J and Kim S U 2014 Human astrocytes: secretome profiles of cytokines and chemokines *PLoS One* **9** e92325
- [55] Flax J D et al 1998 Engraftable human neural stem cells respond to developmental cues, replace neurons, and express foreign genes *Nat. Biotechnol.* **16** 1033–9

- [56] Lee H J, Kim K S, Ahn J, Bae H M, Lim I and Kim S U 2014 Human motor neurons generated from neural stem cells delay clinical onset and prolong life in ALS mouse model *PLoS One* **9** e97518
- [57] Lee H J, Kim K S, Kim E J, Choi H B, Lee K H, Park I H, Ko Y, Jeong S W and Kim S U 2007 Brain transplantation of immortalized human neural stem cells promotes functional recovery in mouse intracerebral hemorrhage stroke model *Stem. Cells* **25** 1204–12
- [58] Lee S R et al 2015 Long-term survival and differentiation of human neural stem cells in nonhuman primate brain with no immunosuppression *Cell Transplant.* **24** 191–201
- [59] Nagai A, Nakagawa E, Hatori K, Choi H B, McLarnon J G, Lee M A and Kim S U 2001 Generation and characterization of immortalized human microglial cell lines: expression of cytokines and chemokines *Neurobiol. Dis.* **8** 1057–68
- [60] Satoh J, Obayashi S, Tabunoki H, Wakana T and Kim S U 2010 Stable expression of neurogenin 1 induces LGR5, a novel stem cell marker, in an immortalized human neural stem cell line HB1.F3 *Cell. Mol. Neurobiol.* **30** 415–26
- [61] Kim S H, Im S-K, Oh S-J, Jeong S, Yoon E-S, Lee C J, Choi N and Hur E-M 2017 Anisotropically organized three-dimensional culture platform for reconstruction of a hippocampal neural network *Nat. Commun.* **8** 1–16
- [62] Kim J A, Kim H N, Im S-K, Chung S, Kang J Y and Choi N 2015 Collagen-based brain microvasculature model *in vitro* using three-dimensional printed template *Biomicrofluidics* **9** 024115
- [63] Yang Y, Leone L M and Kaufman L J 2009 Elastic moduli of collagen gels can be predicted from two-dimensional confocal microscopy *Biophys. J.* **97** 2051–60
- [64] Engler A J, Sen S, Sweeney H L and Discher D E 2006 Matrix elasticity directs stem cell lineage specification *Cell* **126** 677–89
- [65] Chaudhuri O, Gu L, Klumpers D, Darnell M, Bencherif S A, Weaver J C, Huebsch N, Lee H P, Lippens E and Duda G N 2016 Hydrogels with tunable stress relaxation regulate stem cell fate and activity *Nat. Mater.* **15** 326
- [66] Carson M J, Thrash J C and Walter B 2006 The cellular response in neuroinflammation: the role of leukocytes, microglia and astrocytes in neuronal death and survival *Clin. Neurosci. Res.* **6** 237–45
- [67] Chiavari M, Ciotti G M P, Navarra P and Lisi L 2019 Pro-inflammatory activation of a new immortalized human microglia cell line *Brain Sci.* **9** 111
- [68] Ransohoff R M 2016 How neuroinflammation contributes to neurodegeneration *Science* **353** 777–83